TR/6042/C80/04

THE EFFECTS OF REDUCED ATMOSPHERIC PRESSURE ON THERMAL CONTACT RESISTANCE AND ELECTRONIC COMPONENT FORCED AIR FILM COEFFICIENTS

PREPARED BY
CODE 6042
NAVAL WEAPONS SUPPORT CENTER
CRANE, INDIANA 47522

CONTRACT: WRN0016378WR80021

PREPARED FOR
DEPARTMENT OF THE NAVY
NAVAL AVIONICS CENTER
INDIANAPOLIS, INDIANA 46218

(11) 15 Aug 1980

(10) Ronald B./Lannan
Robert/Evan

(6)

THE EFFECTS OF REDUCED ATMOSPHERIC PRESSURE ON THERMAL CONTACT RESISTANCE AND ELECTRONIC COMPONENT FORCED AIR FILM COEFFICIENTS.

Naval Weapons Support Center
Crane, Indiana

(12) 68

(9) Technical Report No.
(14) NWSC/CR/TR/6042/C80/04

409351

FOREWORD

This report was prepared in response to the Modular Avionics Packaging/Standard Avionics Module (MAP/SAM) Program tasking from the Naval Avionics Center, Indianapolis, Indiana in accordance with Work Request N0016378WR80021. The task accomplishments reported herein partially satisfy the requirements of Task II as defined in the subject Work Request.

The writers wish to acknowledge the contributions of Larry Nash for his efforts in the overall guidance and technical support of this task.

Prepared by: Ronald B. Lannan

Ronald B. Lannan
Manager,
Systems Packaging
Design Branch

Robert Evans

Robert Evans
Mechanical Engineer

Approved by: _____

Dean A. Winkler
Manager, Systems
Engineering Division

Approved by: _____

David M. Reece
Electronics System
Engineering Department

ABSTRACT

This report summarizes the theoretical and empirical analysis performed by Naval Weapons Support Center to determine the effects of reduced atmospheric pressure (for altitudes up to 70,000 feet) on conduction and convection thermal interfaces encountered in unpressurized avionics electronic equipment bays. For the purpose of this report the conduction thermal interface of the Improved Standard Electronic Module (ISEM) was selected for study, although the empirical results and theoretical approach revealed herein can be applied to similar conduction interfaces on other electronic modules. The results of the effects of reduced atmospheric pressure on forced-air film coefficients can be applied generally to forced-air cooling of most electronic equipment.

The primary outputs of this report are as follows:

1. A description of the mechanisms associated with rarefied gas phenomenon as related to electronic equipment conduction and convection interfaces.
2. The theoretical results of reduced atmospheric pressure effects on an ISEM guide rib conduction interface with varying contact pressure, surface roughness, and guide rib/card guide materials.
3. An analysis of air property variations with pressure and temperature.
4. The experimental results of reduced atmospheric pressure testing on selected SEM and ISEM guide rib conduction interfaces with varying contact pressure.
5. The theoretical results of reduced atmosphere pressure effects on electronic equipment forced air film coefficients.

TABLE OF CONTENTS

SECTION I

CONCLUSIONS

A. Reduced atmosphere pressure due to increases in altitude can severely degrade thermal performance across metal-to-metal conduction interfaces. Theoretical analysis reveals that the thermal contact resistance of smooth surfaces at 70,000 feet can be up to 2.72 times that at sea level. For rough surfaces the resistance at 70,000 feet can be up to 1.24 times that at sea level. Empirical results of tests performed on an ISEM guide rib interface correlate well with the theoretical analysis and reveals thermal resistance increases of roughly 30% to 50% for conventional SEM and ISEM heat sink frame surface finishes.

B. Thermal contact resistance is strongly dependent on material surface finish at all atmospheric pressures between sea level and 70,000 feet. At sea level the thermal contact resistance of a 125 microinch finish can be up to 6 or 7 times that of a 16 microinch finish. At 70,000 feet altitude the contact resistance of a 125 microinch finish will range up to 3 times that of a 16 microinch finish. This noted dependency is nearly unaffected by varying contact pressures in the range of 25-150 PSI.

C. Thermal contact resistance is moderately dependent on interface contact pressure at all altitudes and, generally, thermal contact resistance for rough contact surfaces is a slightly stronger function of contact pressure than it is for smooth contact surfaces. Considering both smooth and rough contact surface finishes, the thermal contact resistance at 25 PSI will range from 1.25 to 1.68 times that at 150 PSI.

D. The thermal contact resistance of anodized aluminum is significantly higher than that of bare aluminum when mated with a bare aluminum surface. Thermal contact resistance increases due to the anodize (aluminum oxide) coating range from 27% to 45% for SEM guide rib interfaces and from 22% to 64% for ISEM guide rib interfaces. This effect was noted through comparison of experimental data and includes the effects of reduced atmospheric pressure.

E. In examining variations in the properties of atmospheric air between sea level and 70,000 feet altitude, only density and molecular mean free path vary significantly with pressure. Thermal conductivity, dynamic viscosity, and mean molecular speed are practically a pure function of temperature. The specific heat of air is nearly independent of temperature and pressure for the range of temperatures and pressures examined herein.

F. Considering equal mass flows of air at both sea level and 70,000 feet altitude conditions, the convective heat transfer film coefficient, h, will virtually be unaffected (for the same temperature air). For the same conditions of mass flow and temperature, the static pressure loss across heat exchange surfaces will increase dramatically from sea level to 70,000 feet altitude in direct proportion to the density ratio. For these conditions static pressure loss will increase by a factor of 3.35 at 30,000 feet altitude and by a factor of 23.18 at 70,000 feet altitude when compared to sea level operation.

SECTION II

RAREFIED GAS PHENOMENON IN CONDUCTION AND CONVECTION

2.0 INTRODUCTION

Most thermal designers of electronic equipment are accustomed to analyzing fluid properties within the continuum flow regime, where we can effectively average properties over the molecules present and use a macroscopic approach. However, at low pressures, the molecules no longer behave like a continuum and there is a need to consider the motions of individual molecules. For example, at 70,000 feet altitude and a temperature of $15^{o}C$ the average distance traveled by an air molecule before striking another (i.e., mean free path) is 5.84×10^{-5} inches whereas, at sea level and at a temperature of $15^{o}C$, the mean free path decreases to 2.54×10^{-6} inches. At very low pressures, on the order of 10^{-6} atmospheres, the mean free path at $15^{o}C$ increases to about 0.021 inches.

When the mean free path becomes comparable or greater in length than the air gap thickness across conduction interfaces, or greater than the boundary layer thickness or characteristic body dimension at convection interfaces, one cannot analyze the heat transfer problem based on continuum flow but must consider the interaction between individual molecules and the surface under examination. It is the intent of this section to provide very basic guidelines and relationships to show some of the effects that take place in rarefied gases.

2.1 NONCONTINUUM EFFECTS

In order to analyze noncontinuum effects in rarefied gases, it is necessary to divide molecular transport processes into regimes based on the ratio of the molecular mean free path and the physical scale of the transport process. The physical scale may be a boundary layer thickness, an effective air gap thickness, or a characteristic body dimension depending on the type of flow phenomenon being considered. This dimensionless ratio, as referenced above, is called the Knudsen number (Kn). Continuum flow results for small values of this number. For large values of this number, molecular collisions occur primarily at the surface and at large distances from the surface, in the undisturbed stream. This results in "free motion" of the molecules between the surface and the remote fluid and, thus, is called the free-molecule flow regime. Between the continuum and free-molecule regimes is a transition region where the mean free path initially becomes significant and the gas velocity at the wall is no longer zero; this is called the slip flow regime because it can be analyzed by accounting for temperature and velocity "slip" at the gas-solid interface with the remainder of the flow treated by the continuum flow equations.

The Knudsen number, Kn, as mentioned earlier is the parameter of principal interest in defining which regime the molecular transport phenomenon occurs. The Knudsen number is expressed as:

$$Kn = \lambda/L \quad \text{(equation 2-1)}$$

Where: λ = Molecular mean free path

L = Characteristic physical dimension

This form of the Knudsen number is convenient to use when there is no net flow and only conduction in the physical process. In cases where net flow exists, the following form of the Knudsen number is of interest:

$$Kn = \left(\frac{\pi\gamma}{2}\right)^{1/2} \frac{M}{Re} \quad \text{(equation 2-2)}$$

Where: $\gamma = \frac{Cp}{Cv}$ = gas specific heat ratio

M = Mach number (conventional flow parameter)

Re = Reynolds number (conventional flow parameter)

The mean free path, λ, for use in equation 2-1 can be calculated based on the kinetic theory of gases as follows:

$$\lambda = \frac{0.707}{4\pi r^2 n} \quad \text{(equation 2-3)}$$

Where: r = Effective molecular radius for collisions

n = Molecular density

An approximate relation for the mean free path of air molecules is given by:

$$\lambda = 8.64 \times 10^{-7} \, T/P \quad \text{(equation 2-4)}$$

Where: T = gas temperature in ^{o}R

P = gas pressure in lb/ft^2

The Knudsen number ranges which have been generally observed to bound the continuum, slip flow, and free-molecule flow regimes are indicated below. It should be noted, however, that these regimes have not been precisely defined nor universally accepted by experts in rarefied gas phenomenon.

FLOW REGIME	KNUDSEN NUMBER RANGE
Continuum flow	$Kn < 0.001$
Slip flow	$0.001 < Kn < 2$
Free-molecule flow	$Kn > 2$

Study of the above Knudsen numbers reveals that if the characteristic physical dimension is approximately 1000 times greater than the mean free path, continuum flow exists and the heat transfer and fluid flow processes can be handled conventionally. If, however, the characteristic dimension is less than 1000 times the mean free path, one must resort to special flow characterization criteria for slip flow and free-molecule flow.

When molecular transport processes pass from the continuum flow into the slip flow regime a temperature "slip" arises as a result of the failure of the gas molecules to "accommodate" to the surface temperature of the solid. The parameter which describes this behavior is known as the thermal accommodation coefficient, α, defined by:

$$\alpha = \frac{Ei-Er}{Ei-Ew} \quad \text{(equation 2-5)}$$

Where: Ei = Energy of incident molecules on a surface

Er = Energy of molecules reflected from a surface

Ew = Energy molecules would have if they acquired energy of wall at temperatures

Study of this equation reveals that α is the ratio of the actual surface energy interchange to the maximum possible surface energy interchange. For continuum flow α = 1.0 on any surface. For noncontinuum flow α is found to vary with surface material, surface finish, and the gas involved. Table 2-1 lists thermal accommodation coefficients for air and various surfaces. Reference (1) provides an analysis technique for calculating the temperature "slip" at gas-solid interfaces by employing the accommodation coefficient, the mean free path, specific heat ratio, and the Prandtl number. For those interested primarily in velocity "slip" (instead of temperature "slip") at a surface, a reflection coefficient, σ, is used and reference (2) provides the appropriate information for analysis.

TABLE 2-1

THERMAL ACCOMMODATION COEFFICIENTS FOR AIR

Surface Description	α	Surface Emissivity
Flat black lacquer on bronze	0.88 - 0.89	0.93
Bronze, polished	0.91 - 0.94	0.10
Bronze, machined	0.89 - 0.93	0.11
Bronze, etched	0.93 - 0.95	0.19
Cast iron, polished	0.87 - 0.93	0.18
Cast iron, machined	0.87 - 0.88	0.39
Cast iron, etched	0.89 - 0.96	0.70
Aluminum, polished	0.87 - 0.95	0.09
Aluminum, machined	0.95 - 0.97	0.22
Aluminum, etched	0.89 - 0.97	0.78

In the free-molecule flow regime, molecular transport rates are calculated directly from considerations of molecular motion, and the methods of the kinetic theory of gases are used. Here, the net heat transfer rate is the difference between the translational, rotational, and vibrational energy content of the incident and reflected molecules, and the effect of molecular collisions is neglected. The use of a modified Stanton number St', and a modified recovery factor, b', is employed in free-molecule heat transfer. Both of these quantities are dependent upon geometry and treatment of this subject is too detailed for inclusion in this report. Reference (4), however, provides excellent technical information for free-molecule heat transfer from various body geometries.

2.2 CONDUCTION ACROSS UNIFORM AIR GAPS

In order to gain an understanding of the effect that small air gap thicknesses may have on conduction interfaces in reduced atmospheric environments, consider the extreme case where no metal-to-metal contact exists and all heat transfer occurs by conduction through a uniform air gap. Radiation effects are also neglected. In reality there will normally be metal-to-metal conduction and conduction across air gaps acting together, where the air gap conduction represents a portion of the total heat transfer across the interface. This condition is addressed in Section IV. But for now, let's consider only the effects of reduced atmosphere on the conduction across the air gap. Reference (3), equation 12-24, presents a theoretical relationship for the rate of heat transfer across two parallel flat plates with an intersticial uniform air gap. Rearranging terms for thermal resistance, this relationship is as follows:

$$\theta = \frac{\Delta T}{q} = \frac{X\left[1 + \frac{4}{Npr}\frac{\lambda m}{X}\frac{2-\alpha}{\alpha}\frac{\gamma}{\gamma+1}\right]}{KA} \quad \text{(equation 2-6)}$$

Where: θ = Thermal resistance across gap (^{o}C/watt)

Npr = Prandtl number for air = 0.709

λm = Mean free path (inches)

X = Uniform air gap thickness (inches)

α = Accommodation coefficient

γ = Specific heat ratio (1.40 for air)

K = Thermal conductivity of air (watts/in-^{o}C)

A = Cross-sectional area normal to heat flow path (in^{2})

Looking at a specific case where a single ISEM guide rib (A = 0.185 in^2) has a uniform air gap ranging from 0.0005" to 0.003" between itself and an aluminum card guide and where the intersticial air is at 50°C, it is a relatively simple process to determine the thermal resistance across the air gap at various altitude conditions. Table 2-2 shows this thermal resistance across uniform air gaps under conditions of varying altitude and varying air gap thicknesses. Also shown in this table are values for the Knudsen number (Kn) and the mean free path (λm). Examination of the Knudsen number reveals that all values are greater than 0.001 and indicates that conditions for "slip flow" exist, even at sea level conditions. As a result, the accommodation coefficient, α, must then be employed for conditions of aluminum in air. The value of α used in this analysis was taken as 0.90. The mean free path of air, λ m, was calculated as follows, yielding a more accurate solution than that expressed by equation 2-4:

$$\lambda m = 2\nu/\bar{v} \quad \text{(equation 2-7)}$$

Where: ν = Kinematic viscosity (ft^2/sec)

$\bar{v}$ = Mean molecular velocity (ft/sec)

The kinematic viscosity, ν, is the ratio of dynamic viscosity (μ) and density (ρ), and mean molecular velocity ($\bar{v}$) is directly proportional to the square root of temperature for a given gas. Property values and relationships for μ, ρ, and $\bar{v}$ are presented in Section III.

Examination of Table 2-2 reveals that the largest <u>proportional</u> increases in thermal resistance for a given air gap thickness occur at the smaller air gaps. For an air gap thickness of 0.0005", an increase from 3.98 to 8.02°C/watt (102% increase) is noted from sea level to 70,000 ft. Likewise, proportional thermal resistance increases of 52%, 26% and 18% are noted for uniform air gaps of 0.001", 0.002" and 0.003" respectively between sea level and 70,000 ft.

Table 2-2

THERMAL RESISTANCE ACROSS UNIFORM AIR GAP

X(IN)	Kn	λ m (IN)	Altitude (FT)	θ ISEM (^{o}C/Watt)
0.0005	0.0061	3.044×10^{-6}	Sea Level	3.98
0.0005	0.0089	4.432×10^{-6}	10,000	4.06
0.0005	0.0205	1.024×10^{-5}	30,000	4.42
0.0005	0.0533	2.665×10^{-5}	50,000	5.42
0.0005	0.1386	6.931×10^{-5}	70,000	8.02
0.0010	0.0030	3.044×10^{-6}	Sea Level	7.78
0.0010	0.0044	4.432×10^{-6}	10,000	7.86
0.0010	0.0102	1.024×10^{-5}	30,000	8.21
0.0010	0.0266	2.665×10^{-5}	50,000	9.21
0.0010	0.0693	6.931×10^{-5}	70,000	11.81
0.0020	0.0015	3.044×10^{-6}	Sea Level	15.36
0.0020	0.0022	4.432×10^{-6}	10,000	15.45
0.0020	0.0051	1.024×10^{-5}	30,000	15.80
0.0020	0.0133	2.665×10^{-5}	50,000	16.80
0.0020	0.0346	6.931×10^{-5}	70,000	19.40
0.0030	0.0010	3.044×10^{-6}	Sea Level	22.96
0.0030	0.0015	4.432×10^{-6}	10,000	23.04
0.0030	0.0034	1.024×10^{-5}	30,000	23.39
0.0030	0.0088	2.665×10^{-5}	50,000	24.39
0.0030	0.0231	6.931×10^{-5}	70,000	26.99

As expected, the larger air gap thicknesses result in higher thermal resistances, but the effect of altitude for a given air gap thickness is interesting to study. For decreasing air gap thicknesses high values of Kn result and fewer molecular collisions occur within the gap for a given altitude condition. As altitude increases there is a further reduction in molecular collision due to lower air densities. The effect of this is a greater proportional increase in thermal resistance (with increasing altitude) for smaller air gap thicknesses. This effect is important to note and will also be seen in the study of metal to metal conduction interfaces in Section IV.

SECTION III

AIR PROPERTY VARIATIONS WITH TEMPERATURE AND PRESSURE

3.0 INTRODUCTION

The variations in the properties of air becomes an important factor to thermal designers when analyzing the effects of reduced atmospheric conditions on conduction and convection interfaces. The intent of this section is to provide basic relationships and reference data showing the variations of air properties with temperature and pressure. Selected air properties have been evaluated at atmospheric pressures between sea level and 70,000 feet since this is the basic altitude window within which most military avionics equipment must operate. Because most avionics electronic equipments in unpressurized compartments receive temperature-conditioned air, the U. S. Standard Atmosphere values of temperature corresponding to a given altitude are not used in construction of the air properties of Table 3-1. Rather, a value of $15^{o}C$ has been used to evaluate air properties and is judged to be representative of a typical environmental control system coolant supply temperature. Defining equations contained herein will allow evaluations of air properties at other temperatures if so desired.

3.1 AIR PROPERTY VARIATIONS

The following properties of air can be evaluated using the relationships shown. If a given property does not vary significantly with temperature or pressure, it will be so stated. The relationships shown are valid only within the range of temperatures or altitudes (pressures) specified.

Density. The density of atmospheric air varies with both temperature and pressure according to the following relationship:

$$\rho = \frac{P}{RT} \quad \text{(equation 3-1)}$$

Where: ρ = air density (lb/ft^3)

P = Absolute pressure (lb/ft^2)

T = Absolute temperature (^oR)

R = Air gas constant = 53.35 ft-lb/lb_m-^oR

The above relationship is an expression of the perfect gas law and can be used with little error between sea level and 70,000 feet altitude according to reference (6).

Thermal Conductivity. The thermal conductivity of air varies only with temperature at atmospheric conditions between sea level and 70,000 feet and can be expressed as follows:

$$k = \frac{6.325 \times 10^{-7} T^{3/2}}{T + 245.4 \times 10^{-(12/T)}} \quad \text{(equation 3-2)}$$

Where: k = Thermal Conductivity (k-cal/m-sec-^oK)

T = Absolute Temperature (^oK)

Thermal conductivity becomes a significant function of pressure only at altitudes above 300,000 feet where it decreases with increasing altitude.

Dynamic Viscosity. The dynamic viscosity of atmospheric air varies only with temperature between sea level and 70,000 feet altitude and is empirically expressed as follows:

$$\mu = \frac{BT^{3/2}}{T + S} \quad \text{(equation 3-3)}$$

Where: μ = Dynamic viscosity (kg/m-sec)

B = Empirical Constant = 1.458×10^{-6} kg/m-sec-$^{o}K^{1/2}$

T = Absolute Temperature (^{o}K)

S = Sutherland's Constant = $110.4^{o}K$ (exact)

Equation 3-3 becomes invalid for thin layers of air (objects that are small relative to mean path of air) above 100,000 feet and for all situations above 300,000 feet altitude.

Specific Heat. The specific heat of air, (Cp) is nearly independent of temperature in the range of $-200^{o}F$ to $200^{o}F$ varying only about 0.4 percent. Also, for temperatures less than $2500^{o}F$, there is no effect of pressure on the specific heat of air.

Mean Free Path. The molecular mean free path of air is a function of both temperature and pressure as expressed by the following relationship:

$$\lambda m = 8.64 \times 10^{-7} \, T/P \quad \text{(equation 3-4)}$$

Where: λm = Mean Free Path (ft)

T = Air Temperature (^{o}R)

P = Air Pressure (lb/ft^2)

Mean Molecular Speed. The mean molecular speed of air molecules is related to the mean free path, density, and dynamic viscosity as follows:

$$\bar{v} = \frac{2\mu}{\rho \lambda m} \quad \text{(equation 3-5)}$$

Where: $\bar{v}$ = Mean molecular speed (ft/sec)

μ = Dynamic viscosity (lb/ft-sec)

ρ = Density (lb/ft^3)

λm = Mean free path (ft)

3.2 TABULATED VALUES OF AIR PROPERTIES

Table 3-1 reveals the effects of reduced atmospheric pressure on the foregoing properties of air. Atmospheric pressures corresponding to the stated altitude conditions were taken from reference (4). All properties have been evaluated at $15^{o}C$ although evaluation at other given temperatures can be made.

Table 3-1

TABULATED AIR PROPERTIES

Altitude (FT)	ρ (LB/FT^3)	k (BTU/HR-FT^2 -^{o}F/FT)	μ (LB/FT-SEC)	C_p (BTU/LB-^{o}F)	λ_m (FT)	$\bar{v}$ (FT/SEC)	P (LB/FT^2)
Sea Level	0.0765	0.01464	1.202×10^{-5}	0.240	2.12×10^{-7}	1482	2115.36
10,000	0.0527	0.01464	1.202×10^{-5}	0.240	3.08×10^{-7}	1482	1455.01
30,000	0.0228	0.01464	1.202×10^{-5}	0.240	7.11×10^{-7}	1482	629.41
50,000	0.0087	0.01464	1.202×10^{-5}	0.240	1.86×10^{-6}	1482	241.19
70,000	0.0033	0.01464	1.202×10^{-5}	0.240	4.87×10^{-6}	1482	91.91

All properties evaluated at 15^{o}C

SECTION IV

THEORETICAL ANALYSIS OF VARIATIONS IN IMPROVED SEM GUIDE RIB THERMAL CONTACT RESISTANCE WITH REDUCED ATMOSPHERIC PRESSURE

4.0 INTRODUCTION

Survey of the technical literature on predicting thermal contact resistances revealed several theoretical approaches to the subject but few of these theoretical approaches were supported by experimental test results. The most promising approach found for predicting thermal contact resistances was a correlation established by T. Nejat Veziroglu of the University of Miami, Coral Gables, Fla. In a report entitled "Correlation of Thermal Contact Conductance Experimental Results" (reference (5)), Professor Veziroglu outlines a procedure for estimating thermal contact conductances (or resistances) based on correlations with the experimental results of several researchers. The correlations were carried out over a wide range of variables including contact materials, intersticial fluids, surface finishes and roughnesses, contact pressure, temperatures, and conductances. Although the correlation of reference (5) did not originally cover experiments in a vacuum, later work by Professor Veziroglu showed that this correlation yielded excellent results for both partial and full vacuum experiments, especially using air as the intersticial fluid between contact materials. Conversations with Professor Veziroglu during December 1979 revealed that a report was being written to summarize the results of the subject correlation for reduced pressure situations and would be available sometime in 1980.

The Veziroglu correlation established in reference (5), hereinafter referred to as the "V" correlation, is also presented in reference (2) in a shorter form for quick, practical application. The use of reference (2) along with this report will allow the thermal designer to predict thermal contact resistances without requiring extensive investigation for definition of terms or for the various material/geometry input parameters.

The "V" correlation was performed by means of a digital computer whereby a theoretical contact conductance equation was utilized and the various input parameters to the equation were calculated from experimental results. Input parameters included effective fluid gap thickness, constriction number, gap number, and equivalent conductivity of intersticial fluid. The results of the "V" correlation cover metal contacts with an intersticial fluid between them. A total of 76 experiments comprised the data base for the correlation. Air was the intersticial fluid in 58 of the 76 experiments and other intersticial fluids included argon, helium, water, glycerol, lubricating oil, and paraffin. The contact materials were comprised of aluminum to aluminum (in air) for 20 experiments, either steel to steel or stainless steel to stainless steel (in air) for 16 experiments, brass to brass (in air) for 6 experiments, and combinations of the aforementioned metals in air for 10 experiments. As can be seen, the resulting correlation was heavily biased toward air as the intersticial fluid with either aluminum or steel as the contacting metals. Other metals covered by the correlation included iron, bronze, gun metal, uranium, and magnox. Surface finishes of the metals covered by the experiments ranged from 3 to 3300 microinches although all of the aluminum and stainless steel surface finishes represented were between 10

and 120 microinches. Contact pressures encompassed by the experimental data ranged from 2.5 to 20,000 PSI, mean contact temperatures ranged from 27°C to 320°C, and metal hardnesses ranged from 10,000 to 350,000 PSI (Meyer's hardness).

Use of the "V" correlation described herein will result in a mean deviation of approximately ± 35% in the predicted value of thermal contact conductance (compared to experimental results) and the maximum deviation will be on the order of two. Although not outstanding, considering the wide range of contact materials, surface finishes, contact pressures and temperatures, the degree of correlation obtained using this method is good. A correlation of much narrower scope would greatly aid those interested in specific materials or ranges of input parameters.

4.1 APPLICATIONS OF THE "V" CORRELATION TO ISEM GUIDE RIB INTERFACES

For the purpose of this report a single ISEM guide rib thermal interface will be examined to predict the thermal contact resistance. The guide rib itself is assumed to be made of alloy 5052 aluminum, anodzied to a thickness of approximately 0.0004 inches, and has an apparent contact area of 0.185 in^2 with the mating card guide. The card guide material is also assumed to be alloy 5052 aluminum anodized to a thickness of 0.0004 inches. The above card guide and guide rib materials are common in the SEM program, although other materials may be analyzed using the prediction method described herein.

The "V" correlation method will be used to predict the thermal contact resistance between the guide rib and the card guide with the following parameters independently and discretely varied as specified:

a. Contact pressures: 25-50-100-150 PSI

b. Altitude conditions: SL-10,000-30,000-50,000-70,000 feet

c. Surface finish: 16-32-64-125 microinches

The mean interface temperature between the two contact materials is assumed to be $50^{o}C$ for this analysis.

4.2 PROCEDURE FOR USING "V" CORRELATION METHOD

The procedure for using the "V" correlation method to predict thermal contact resistances is shown below. The specific values calculated for various input parameters are applicable only for the ISEM guide rib thermal interface as described in Section 4.1 although the general procedure is applicable for predicting contact resistances of other configurations and imput parameter variables.

STEP 1 - Calculate Constriction Number C

$$C = (p/M)^{1/2} \qquad \text{(Equation 4-1)}$$

p = Apparent contact pressure (PSI)

M = Meyer hardness (PSI) of the softer contact material

Meyer hardness (M) is addressed in reference (6) and is normally within 7% of the Brinell hardness. Knowing the Brinell hardness number (BHN) in kilograms/mm^2 plus the size of load and the diameter of the ball used in the hardness test, one can calculate Meyer hardness by determining the diameter of the impression on the material being tested. Brinell hardness is given as:

$$BHN = \frac{P}{\pi D/2 \left(D-(D^2-d^2)^{1/2}\right)} \quad (kg/mm^2)$$

Where P = Load (kg)

D = Diameter of ball (mm)

d = Diameter of indentation (mm)

Solving for d, the diameter of the indentation:

$$d = \left[D^2-\left[\frac{2P}{\pi D\, BHN} - D\right]^2\right]^{1/2}$$

Knowing the diameter of the impression derived from the Brinell hardness number, one can calculate the Meyer hardness number as follows:

$$M = \frac{4P}{\pi d^2} \quad (kg/mm^2)$$

Where P = Load (kg)

d = Diameter of impression (mm)

Note that Meyer hardness is the load divided by the projected area of the indentation whereas Brinell hardness is the load divided by the surface area of the resulting indentation. For the specific case of aluminum alloy 5052-H34, a Brinell hardness of 68 kg/mm^2 is reported in the literature. Using the foregoing relationships, the Meyer hardness number for this alloy was calculated to be 69.7 kh/mm^2 or 99,084 PSI. This was based on Brinell hardness testing using a 500 kg load and a 10mm diameter ball.

Referring to equation 4-1, values of the constriction number (C) were calculated based on the contact pressures and hardness of the aluminum material assumed in this analysis. Table 4-1 presents values of the constriction number (C) as a function of contact pressure (P).

STEP 2 - Estimate effective gap thickness l

$l = 3.56 (l_1 + l_2)$ if $l_1 + l_2 < 280$ inches (smooth contacts) (equation 4-2)

$l = 0.46 (l_1 + l_2)$ if $l_1 + l_2 > 280$ inches (rough contacts) (equation 4-3)

Where: l_1 = Mean or rms depth of surface roughness for contact material #1

l_2 = Mean or rms depth of surface roughness for contact material #2

The effective gap thickness is the effective distance between the contact surfaces from the heat transfer point of view and the sum of the mean roughness depths of the two contact surfaces as measured by a surface analyzer. The method of contact surface finish (i.e. lapping, grinding, etc.) has little or no effect on l and, due to "V" correlation data scatter, was not determined to be a significant factor. Equation 4-2 shows that l is greater

than $l_1 + l_2$, meaning that the order of waviness or macroroughness is greater than the order of microroughness (as measured by surface analyzers) and that macroroughness governs the gap thickness. In contrast, equation 4-3 (for rough contacts), shows that l is less than $l_1 + l_2$, meaning that rough surfaces can be machined within relatively (percentage-wise) closer limits. Reference (5) provides more discussion on this topic for the interested reader.

Table 4-2 gives effective gap thicknesses, l, corresponding to the surface finishes chose for the ISEM guide rib analysis.

STEP 3 - Calculate Gap Number B

$$B = 0.335\ C^{0.315\,(\sqrt{A}/l)^{0.137}} \qquad \text{(equation 4-4)}$$

Where C = Constriction number

A = Contact interface area (in^2)

l = Effective gap thickness (in)

Examination of equation 4-4 reveals that the gap number is a function of contact pressure, material hardness, effective gap thickness (surface finish), and interface area. Many combinations of contact pressures and material surface finishes were used in the subject ISEM guide rib analysis and are shown in Table 4-3. The interface area (A) used in this analysis is taken as 0.185 in^2 and is the contact area of one ISEM guide rib with the card guide.

STEP 4 Calculate equivalent conductivity (k_f) of intersticial fluid evaluated at mean surface temperatures $\overline{t_i} = (t_1 + t_2)/2$

For gases, the equivalent conductivity is expressed as follows:

$$k_f = \left[\frac{k_o}{1 + 8\gamma(\nu/\bar{v})(a_1 + a_2 - a_1 a_2)/Pr(\gamma + 1)la_1 a_2} + \frac{4\sigma l \epsilon_1 \epsilon_2 \overline{t_i}^3}{\epsilon_1 + \epsilon_2 - \epsilon_1 \epsilon_2} \right] \qquad \text{(equation 4-5)}$$

Where: k_o = Gas conductivity at zero contact pressure (BTU/hr-ft-^oF)

γ = Specific heat ratio (1.4 for air)

ν = Kinematic viscosity of gas evaluated at $\overline{ti}$(ft^2/hr)

$\bar{v}$ = Mean molecular gas velocity (ft/hr)

a_x = Accomodation coefficient of each contact material

Pr = Prandtl number (0.69 - 0.71 for air)

l = Effective gap thickness (ft)

σ = Stefan-Boltzmann radiation constant (σ = 17.3 X 10^{-10} BTU/hr-ft^2-$^oR^4$)

$\overline{t_i}$ = Mean interface temperature of contacts (^oR)

ϵ_x = Emissivity of respective contact surface

Proper evaluation and understanding of equation 4-5 is essential for successful application of the "V" correlation, so some discussion will hereby be presented to provide sufficient detail for analysis.

Equation 4-5 includes material and gas property terms that account for radiation effects between contact materials and for reduced gas pressure. The portion of the equation that contains the radiation constant (σ) and the emissivities (ϵ) of the materials accounts for the radiation heat flow between the contact materials. Emissivity of anodized aluminum was used in this

analysis and was assumed to be 0.90. The radiation heat transfer described by equation 4-5 is shown to vary directly with effective gap thickness (l) and must be evaluated for each contact surface finish. As shown by equation 4-5, as l increases, the portion of radiation heat flow increases directly and the conduction heat transfer across the intersticial air gap decreases accordingly by constant $\div \left(1 + \frac{\text{CONSTANT}}{l}\right)$. The gas conductivity at zero contact pressure (k_o) is evaluated at $\bar{t}_i$ and is independent of gas pressure within the scope of this analysis (see equation 3-2). The kinematic viscocity (ν) is a function of both pressure and temperature and must be evaluated for each variation thereof (note that ν = dynamic viscosity (μ) divided by density (ρ) and can be evaluated by equations 3-1 and 3-3). The mean molecular velocity ($\bar{v}$) is a function of temperature only and can be evaluated by equation 3-5. It is interesting to note that the term $\nu/\bar{v}$ is equal to $\lambda m/2$ (see equation 2-7) and thus equation 4-5 accounts for the reduced pressure effects of the gas on the mean free path (λm). The accomodation coefficients (a_1 and a_2) should be employed per table 3-1 and for this analysis are taken as 0.90 for anodized aluminum. "Slip flow" will most likely exist under all situations studied in this analysis since the actual resulting intersticial air gap thickness (not effective gap thickness used for the "V" correlation) will be less than 1000 times the mean free path of the air molecules as calculated per equation 3-4.

Table 4-4 presents calculated values of equivalent conductivity (k_f) based on the conditions specified herein for the ISEM guide rib analysis. Note that equivalent conductivity increases with increasing surface roughness due to the "slip flow" effects for small intersticial air gaps between contact materials.

STEP 5 - Calculate Conductivity Number K.

$$K = k_f(k_1 + k_2)/2k_1k_2 \qquad \text{(equation 4-6)}$$

Where: k_f = equivalent conductivity (BTU/hr-ft-^oF)

k_1 = thermal conductivity of contact material #1 (BTU/hr-ft-^oF)

k_2 = thermal conductivity of contact material #2 (BTU/hr-ft-^oF)

K is the ratio of the effective fluid conductivity to the harmonic mean of the thermal conductivities of the contact solids evaluated (for small anticipated interface temperature drops) at the mean contact interface temperature. Since anodized aluminum is being evaluated as the contact material in this analysis, the conductivity of the anodic coating (aluminum oxide) is used to compute K. The conductivity of aluminum oxide is reported in the literature as being 12.51 BTU/hr-ft-^oF (0.55 watts/in-^oC) and substitution of this value for k_1 and k_2 in equation 4-6 shows that, for this specific case, $K = 0.08\ k_f$. Thus, values of K can be determined by multiplying all values of k_f in Table 4-4 by 0.08. In reality the bulk conduction resistance of the anodic coating for the guide rib and card guide surfaces must be added to the constriction resistance (determined by the "V" correlation) since they are in series thermally. However the bulk conduction resistance of the aluminum oxide coating on the contacting surface of an ISEM guide rib ($A = 0.185\ in^2$) is less than 0.01 ^oC/watt and can therefore be neglected.

STEP 6 - Using previously determined parameters B, K, and C, determine the value of h_j, contact conductance per unit area, by one of the following methods:

(a) Calculate the conductance number (U) from equation 4-7 below using iteration (since it is a transcendental equation) and solve equation 4-8 below for h_i.

$$U = 1 + \frac{BC}{K \tan^{-1}\left[(1/C)\sqrt{1-(1/U)}-1\right]} \qquad \text{(equation 4-7)}$$

$$h_i = U k_f / l \qquad \text{(equation 4-8)}$$

Where: h_i = contact conductance per unit are (BTU/hr-ft^2-^{o}F)

U = conductance number

k_f = equivalent conductivity (BTU/hr-ft^2-^{o}F)

l = effective gap thickness (ft)

(b) Find U from a chart presented in Figure 8 of reference (5) or Figure 9, p. 3-17 of reference (2), and then calculate h_i from equation 4-8. These figures are plots of equation 4-7 as U-1 versus B/K for various values of C.

Method (a) above is very time consuming to do manually because it involves many iterations and subsequently was not used for the subject ISEM guide rib analysis. Method (b) is much easier but still involves a lot of graphical "look up" for any sizeable analysis such as this one. After studying the log-log plots of reference (2), figure 9, p. 3-17 and the range of B/K values needed to perform this analysis, it became evident that equations could be fitted to the log-log plots to allow calculation of h_i. For B/K values from roughly 10^{-1} to 10^5 the plot of log $\left(\frac{h_i l}{k_f}-1\right)$ versus log $\left(\frac{B}{K}\right)$ is linear

suggesting that an equation of the form $y = bx^n$ would allow an accurate fit. If we let $y=(\frac{h_i l}{k_f})-1$ and $x = B/K$ then one can determine values for b (a constant) and n (real slope on log-log plot) for various values of the constriction number (C), and the resulting equation becomes:

$$\frac{h_i l}{k_f} - 1 = b(B/K)^n \qquad \text{(equation 4-9)}$$

The slope of the log-log plot (n) from reference (2) was determined to be 1.0 for all values of C within the cited range of B/K values, therefore an equation of the form $y = bx$ will allow calculation of b (by substitution of values for $\frac{B}{K}$ and $\frac{h_i l}{k_f} - 1$) for the various values of C. Solving equation 4-9 for h_i yields:

$$h_i = [b(B/K)+1]\, k_f/l \qquad \text{(equation 4-10)}$$

Table 4-5 gives values of b corresponding to selected values of C for use in equation 4-10. It should be noted, though, that use of equation 4-10 is valid only for the B/K range of values specified in Table 4-5 and that method (b) above must be used for determining h_i for B/K values outside the validity range of the specified values.

4.3 RESULTS OF CONTACT RESISTANCE PREDICTIONS

The results of the predictions on thermal contact resistances for a single, anodized ISEM guide rib are presented in Table 4-6 and cover the ranges of material surface finish, reduced atmospheric pressure (resulting

from increased altitude), and apparent contact pressure previously noted in paragraph 4.2. Values of B/K, C, and equation constant "b" are presented in Table 4-6 and were used in equation 4-10 to calculate the contact conductance per unit area (h_i). The thermal resistance (θ) was calculated from the relationship $\theta = 1/h_i A$, where A is the ISEM guide rib contact surface area (0.185 in^2).

Examination of Table 4-6 reveals the following effects of altitude, material surface finish, and contact pressure on the guide rib thermal interface resistance (θ):

(a) θ is strongly dependent on material surface finish from sea level to 70,000 ft. At sea level θ is reduced by a factor of 6 or 7 times when surface roughness is decreased from 125 μinches to 16 μinches. At 70,000 ft. this effect is less (due to greater "slip flow" effects on smooth contacts) but the reduction in θ is still on the order of 3 times. This dependency of θ on surface roughness is nearly unaffected by increases in contact pressure in the range from 25-150 PSI.

(b) θ is moderately dependent on interface contact pressure at all altitudes and, generally, θ for rough contact surfaces is a stronger function of contact pressure than is θ for smooth contact surfaces. For a given surface finish, increasing contact pressure from 25 to 150 PSI decreases θ by a factor ranging from 1.25 to 1.68 for smooth contacts (16 u inch finish) and by a factor of 1.44 to 1.54 for rough contacts. The effect of higher contact pressure on θ is stronger for

smooth contacts only at altitudes at or above 70,000 ft. where a decrease in θ by a factor of 1.68 is noted. At all altitudes below approximately 70,000 ft., the effect of higher contact pressure on θ is stronger for rough contacts. This phenomenon is evidenced due to the fact that, at very high altitudes, the mean free path of the air molecules is large even for the larger (rough contact) intersticial air gaps and most heat transfer occurs by metal to metal conduction. This, in turn, makes the interface with more metal to metal contact spots (i.e. smooth contacts) a stronger function of contact pressure.

(c) θ is a strong function of altitude for a given contact pressure and smooth contacts show a much greater (percentage-wise) increase in θ with increasing altitude than do rough contacts. This dependency of θ on altitude is weakened slightly by increasing contact pressure from 25 to 150 PSI. From Table 4-6 it is seen that for 25 PSI and a smooth 16 u-inch surface finish θ increases by a factor of 2.72 between sea level and 70,0000 ft. altitude whereas, at 150 PSI, θ increases by a factor of 2.03. Likewise, for a rougher 125 u-inch surface finish and a contact pressure of 25 PSI, θ increases by a factor of 1.24 whereas, at 150 PSI, θ increases by a factor of 1.15. The greater (percentage-wise) increase in θ with altitude for smooth contacts is again explained by the rarefied gas "slip flow" effect for the very thin intersticial air gaps for smooth surfaces.

TABLE 4-1

CONSTRICTION NUMBER - C

CONTACT PRESSURE (PSI)	C
25	1.588×10^{-2}
50	2.246×10^{-2}
100	3.177×10^{-2}
150	3.891×10^{-2}

MATERIAL: Aluminum alloy 5052-H34

MEYER HARDNESS = 99,084 PSI

TABLE 4-2

EFFECTIVE GAP THICKNESS - l

Surface Finish of One Contact Material (μ inches)	l (ft)	l (inches)
16	9.493×10^{-6}	113.92×10^{-6}
32	1.899×10^{-5}	227.84×10^{-6}
64	3.708×10^{-5}	456.00×10^{-6}
125	7.417×10^{-5}	890.00×10^{-6}

$l = 3.56\ (l_1 + l_2)$ for smooth contacts

$l_1 = l_2$ for this analysis

TABLE 4-3

GAP NUMBER - B

Contact Pressure (PSI)	Surface Finish (μIN)*	B
25	16	5.95×10^{-3}
	32	8.57×10^{-3}
	64	1.19×10^{-2}
	125	1.60×10^{-2}
50	16	8.34×10^{-3}
	32	1.16×10^{-2}
	64	1.57×10^{-2}
	125	2.07×10^{-2}
100	16	1.17×10^{-2}
	32	1.58×10^{-2}
	64	2.08×10^{-2}
	125	2.66×10^{-2}
150	16	1.42×10^{-2}
	32	1.89×10^{-2}
	64	2.45×10^{-2}
	125	3.09×10^{-2}

* Applicable to each contact material

TABLE 4-4

EQUIVALENT CONDUCTIVITY - k_f

Altitude (FT)	Surface Finish (μIN)*	Equivalent conductvity - k_f [BTU/hr-ft-°F]
Sea Level	16	0.01464
	32	0.01535
	64	0.01574
	125	0.01598
10,000	16	0.01405
	32	0.01502
	64	0.01555
	125	0.01588
30,000	16	0.01204
	32	0.01379
	64	0.01486
	125	0.01551
50,000	16	0.00857
	32	0.01119
	64	0.01318
	125	0.01455
70,000	16	0.00487
	32	0.00749
	64	0.01015
	125	0.01251

* Surface finish of each contact material

TABLE 4-5

VALUES OF "b" FOR USE IN EQUATION 4-10

Constriction Number - C	b	$\frac{B}{K}$ Valid Range
2×10^{-3}	1.33×10^{-3}	$1 - 10^5$
4×10^{-3}	2.66×10^{-3}	$0.4 - 10^5$
6×10^{-3}	4.00×10^{-3}	$0.1 - 10^5$
8×10^{-3}	5.33×10^{-3}	$0.1 - 10^5$
1×10^{-2}	6.66×10^{-3}	$0.1 - 10^5$
2×10^{-2}	1.333×10^{-2}	$0.01 - 10^5$
4×10^{-2}	2.666×10^{-2}	$1 - 10^5$
6×10^{-2}	4.000×10^{-2}	$1 - 10^5$
8×10^{-2}	5.332×10^{-2}	$1 - 10^5$
1×10^{-1}	6.635×10^{-2}	$1 - 10^5$
2×10^{-1}	1.500×10^{-1}	$1 - 10^5$
4×10^{-1}	4.000×10^{-1}	$10 - 10^5$
6×10^{-1}	1.0000	$10 - 10^5$
8×10^{-1}	3.3333	$10 - 10^5$
9×10^{-1}	8.0000	$10 - 10^5$

$$h_i = [b(B/K)+1][k_f/l] \qquad \text{(equation 4-10)}$$

TABLE 4-6

INTERFACE RESISTANCE AT 25 PSI

$C = 1.588 \times 10^{-2}$
$b = 1.059 \times 10^{-2}$

Altitude (FT)	Finish (μIN*)	$\frac{B}{K}$	$h_i(\frac{watts}{in^2-^oC})$	$\theta(\frac{^oC}{watt})$
SL	16	5.08	5.95	0.91
	32	6.98	3.18	1.70
	64	9.45	1.71	3.16
	125	12.52	0.89	6.05
10K	16	5.29	5.73	0.94
	32	7.13	3.12	1.73
	64	9.57	1.69	3.19
	125	12.59	0.89	6.08
30K	16	6.18	4.95	1.09
	32	7.77	2.88	1.88
	64	10.01	1.62	3.33
	125	12.89	0.87	6.21
50K	16	8.68	3.61	1.50
	32	9.57	2.38	2.27
	64	11.29	1.46	3.71
	125	13.74	0.82	6.57
70K	16	15.27	2.18	2.48
	32	14.30	1.66	3.25
	64	14.65	1.16	4.66
	125	15.99	0.72	7.48

* Surface finish of <u>each</u> contact material

TABLE 4-6 (CONT'D.)

INTERFACE RESISTANCE AT 50 PSI

$C = 2.246 \times 10^{-2}$
$b = 1.5 \times 10^{-2}$

Altitude (FT)	Finish (μIN*)	$\frac{B}{K}$	h_i ($\frac{watts}{in^2 - °C}$)	θ ($\frac{°C}{watt}$)
SL	16	7.12	6.25	0.86
	32	9.45	3.38	1.60
	64	12.47	1.85	2.93
	125	16.19	0.98	5.51
10K	16	7.42	6.03	0.90
	32	9.65	3.32	1.63
	64	12.62	1.83	2.96
	125	16.29	0.97	5.54
30K	16	8.66	5.25	1.03
	32	10.51	3.08	1.75
	64	13.21	1.76	3.07
	125	16.68	0.96	5.64
50K	16	12.16	3.91	1.38
	32	12.95	2.58	2.10
	64	14.89	1.59	3.39
	125	17.78	0.91	5.94
70K	16	21.40	2.48	2.18
	32	19.36	1.86	2.90
	64	19.33	1.29	4.18
	125	20.69	0.81	6.68

TABLE 4-6 (CONT'D.)

INTERFACE RESISTANCE AT 100 PSI

$C = 3.177 \times 10^{-2}$
$b = 2.11 \times 10^{-2}$

Altitude (FT)	Finish (μIN*)	$\frac{B}{K}$	$h_i \left(\frac{\text{watts}}{\text{in}^2\text{-}^\circ\text{C}}\right)$	$\theta \left(\frac{^\circ\text{C}}{\text{watt}}\right)$
SL	16	9.99	6.84	0.79
	32	12.87	3.76	1.44
	64	16.52	2.10	2.58
	125	20.81	1.14	4.76
10K	16	10.41	6.61	0.82
	32	13.14	3.70	1.46
	64	16.72	2.08	2.60
	125	20.94	1.13	4.78
30K	16	12.14	5.84	0.93
	32	14.32	3.46	1.56
	64	17.49	2.01	2.69
	125	21.43	1.11	4.86
50K	16	17.06	4.50	1.20
	32	17.64	2.96	1.82
	64	19.73	1.84	2.93
	125	22.85	1.07	5.07
70K	16	30.02	3.07	1.76
	32	26.37	2.25	2.40
	64	25.60	1.54	3.50
	125	26.60	0.96	5.61

TABLE 4-6 (CONT'D.)

INTERFACE RESISTANCE AT 150 PSI

$C = 3.891 \times 10^{-2}$
$b = 2.59 \times 10^{-2}$

Altitude (FT)	Finish (μIN*)	$\frac{B}{K}$	$h_i(\frac{watts}{in^2-°C})$	$\theta(\frac{°C}{watt})$
SL	16	12.12	7.42	0.73
	32	15.39	4.14	1.31
	64	19.46	2.34	2.31
	125	24.18	1.28	4.21
10K	16	12.63	7.20	0.75
	32	15.72	4.08	1.33
	64	19.69	2.32	2.33
	125	24.33	1.28	4.23
30K	16	14.74	6.32	0.84
	32	17.14	3.84	1.41
	64	20.61	2.25	2.40
	125	24.90	1.26	4.29
50K	16	20.71	5.08	1.06
	32	21.10	3.34	1.62
	64	23.24	2.09	2.59
	125	26.55	1.21	4.46
70K	16	36.44	3.65	1.48
	32	31.55	2.63	2.06
	64	30.16	1.79	3.03
	125	30.90	1.11	4.86

SECTION V

EMPIRICAL ANALYSIS OF EFFECTS OF REDUCED ATMOSPHERIC PRESSURE ON SEM AND ISEM THERMAL CONTACT RESISTANCE

5.0 INTRODUCTION

The purpose of this experimental analysis was to determine the effects of contact pressure and atmospheric pressure on the thermal interface resistance between the module guide rib and the card cage for Standard Electronic Modules (SEM) and Improved Standard Electronic Modules (ISEM). In addition the effect of anodization of the module guide ribs on the thermal interface resistance was determined for SEM and ISEM.

Each test module was subjected to contact pressures of 25, 50, 100 and 150 PSI at simulated altitudes of 10,000, 30,000, 50,000 and 80,000 feet in addition to local ambient atmospheric pressure. The temperatures sensed by the thermocouples on the test fixture and the modules were recorded for each combination of contact pressure and altitude.

5.1 DESCRIPTION OF TEST CONFIGURATION

In order to provide a variable amount of contact pressure, a test fixture was designed using four calibrated, squared-end, compression springs. By generating a plot of force versus deflection for the springs, specific contact forces were exerted at the guide rib interface by moving the adjusting nuts (see enclosed drawing 79WQ0810 for test fixture). Adjusting the hex nuts increased or decreased the amount each spring was compressed. The amount of spring compression, and thus the force exerted on the clamp, was determined by measuring the distance between the front clamp and the clamp assembly adjacent to each spring.

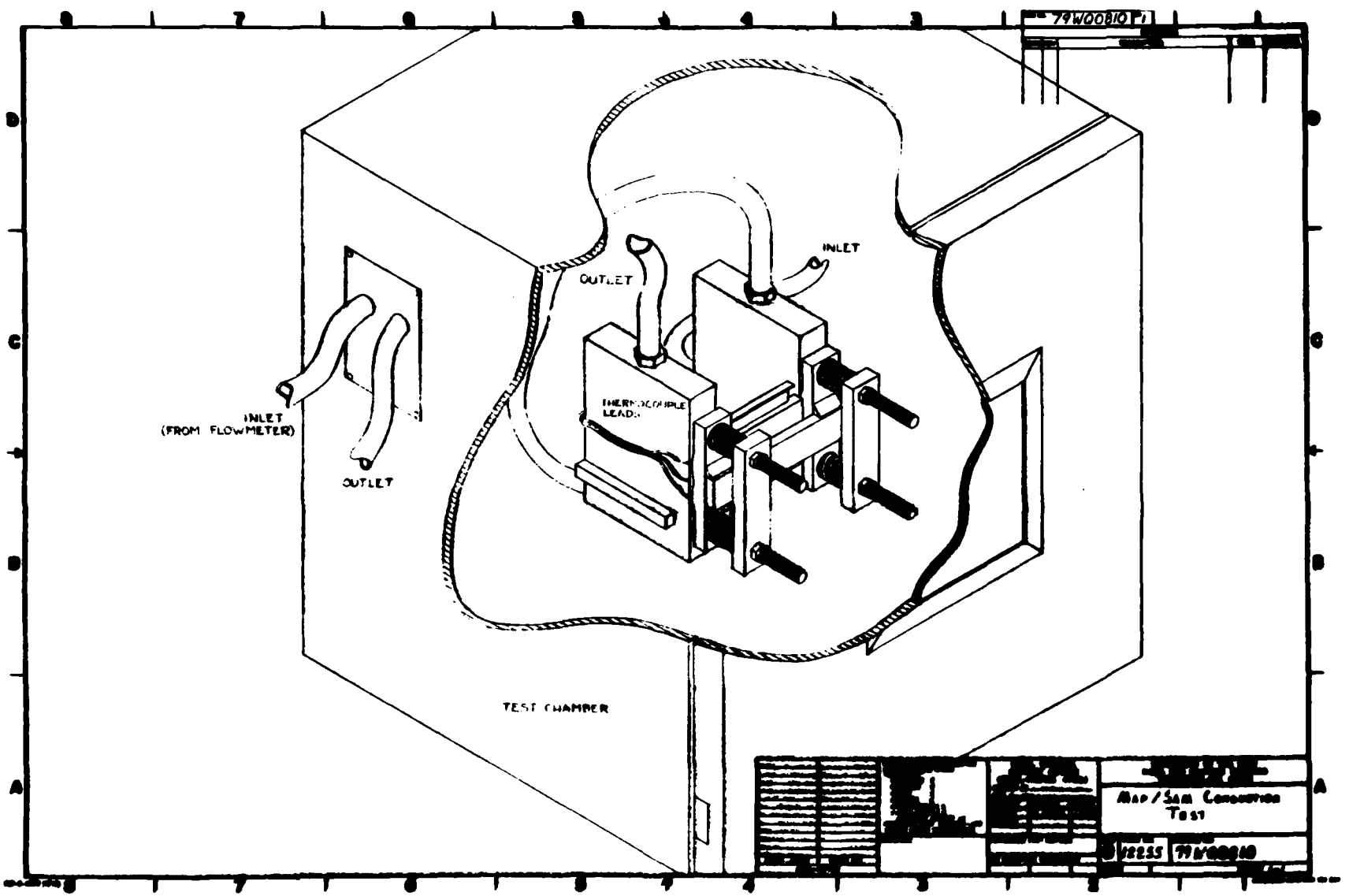
79W00810 P1
INLET
OUTLET
INLET
(FROM FLOWMETER)
OUTLET
THERMOCOUPLE
LEAD
TEST CHAMBER
MAP/SAM Connection
Test

In addition to providing the required clamping force, the test fixture also served as a heat sink for the modules. Each side of the fixture was fabricated with interior passages to permit the flow of coolant through the fixture. Three thermocouples were mounted 0.050 inches from the module-test fixture interface on each half of the fixture. These thermocouples were used to monitor the heat sink temperatures used in calculating the interface thermal resistances.

Test modules of two finishes (untreated and anodized) and two types (SEM and ISEM) were used. All modules utilized aluminum center frame heat sinks (see enclosed drawing 79WQ0801) and were instrumented with two thermocouples on each guide rib. These thermocouples were mounted to the module on the guide rib surface opposite the module-heatsink interface using thermally conductive epoxy adhesive. Each module utilized nine 100 ohm resistors in series to supply the thermal load for the experiment.

5.2 TEST PROCEDURE

The test fixture was installed in the altitude chamber with the test module inserted as shown in enclosed drawing 79WQ0810. After all fluid and electrical connections were completed, the test fixture was visually checked for proper alignment and clearance. After these checks, the hex nuts were adjusted to compress the springs enough to generate the required contact pressure on each guide rib. High contact pressure tests were performed first to eliminate any small surface irregularities which might vary as the contact pressure was increased later in the test. The final step before actual

DWG NO.	SH

REVISIONS			
REV	DESCRIPTION	DATE	APPROVED

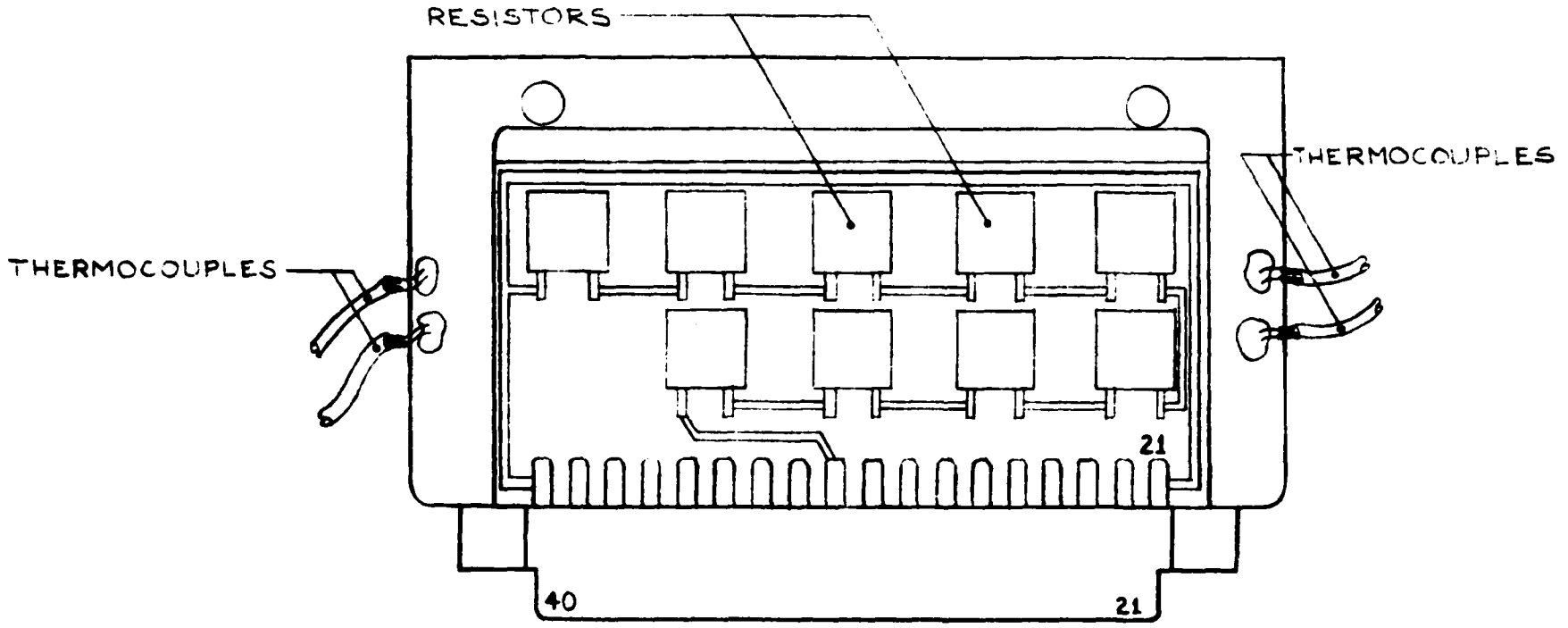

NEXT ASSY	USED ON
APPLICATION	

UNLESS OTHERWISE SPECIFIED
DIMENSIONS ARE IN INCHES
TOLERANCES:
CAPACITANCE ±
RESISTANCE ±
ANGLES ±
FRACTIONS ±
2 PLACE DECIMALS ±
3 PLACE DECIMALS ±
INTERPRET DRAWING IN ACCORDANCE WITH MIL-STD-100
DO NOT SCALE THIS DRAWING

MATERIAL

NAVAL WEAPONS SUPPORT CENTER
CRANE, INDIANA 47522
CONTRACT NO.
DATE

PREPARED	R East	1/3/79
CHECKED		
ENGINEER		

APPROVED FOR NAVSEA
BY DIRECTION COMNAVSEA

DEPARTMENT OF THE NAVY
NAVAL SEA SYSTEMS COMMAND
WASHINGTON, D.C. 20362

INSTRUMENTED MODULE

SIZE	FSCM NO.	DRAWING NO
A		79WQ0801

SCALE NONE

SHEET 1 OF 1

testing was the installation of an aluminum radiation shield. This shield minimized heat radiation to the altitude chamber walls and also convection of heat to the local air. Temperature measurements were made at local atmospheric pressure (29.07 inches of Hg) after the coolant flow rate and the fixture temperature had stabilized. The atmospheric pressure in the test chamber was then changed to simulate atmospheric pressure at altitudes of 10,000, 30,000, 50,000 and 80,000 feet. Data was collected after approximately one minute at each altitude to allow for temperature stabilization of the module and test fixture. The above test procedure was repeated for each contact pressure.

5.3 TEST RESULTS

For the purpose of this test it was assumed that all power dissipated by the module was conducted to the heat sink via the guide ribs. Although this assumption is not completely valid due to re-radiation and natural convection which occured within the radiation shield, the coolant temperature was 12 to 15^{o}F cooler than the test chamber air temperature and the radiation shield should have retarded a very high percentage of the natural convection heat transfer.

The thermal resistance at the module-heatsink interface (θ) was thus determined by dividing the sum of the measured temperature differences between the module guide ribs and the heatsinks by the power dissipated by the module. This is, in effect, the average thermal resistance of a single guide rib interface. To obtain the guide rib to heat sink interface resistance based on two interfaces in parallel, one has to divide this number by two.

Tables 5-1, 5-2, 5-3, and 5-4 present the results of the contact resistance tests performed on unanodized SEM frames, anodized SEM frames, unanodized ISEM frames, and anodized ISEM frames, respectively. The guide rib interface resistance (θ) presented in these tables is the average thermal resistance across a single guide rib interface based on data averaged over two guide rib interfaces. The average combined surface finish denoted in the tables was determined by making surface profilometer measurements on two guide ribs and two bare aluminum heat sink fixture surfaces and is representative of the sum of the averaged surface finishes for both the guide rib and the heatsink.

5.4 EFFECTS OF ANODIZED COATING ON THERMAL RESISTANCE

The thermal conductivity of aluminum oxide is approximately one tenth that of higher conductivity aluminum alloys and, as a result, increases the thermal constriction resistance across metal contact interfaces. This is seen by perusing the data contained in Tables 5-1 through 5-4 and noting the higher thermal interface resistance for anodized heat sink frames compared to those for bare aluminum. Table 5-5 shows the ratio of anodized guide rib interface resistance to that of bare aluminum for both SEM and ISEM interfaces. From this table it is seen that the resistance of anodized guide rib interfaces is signficantly higher those of bare aluminum. By averaging these resistance ratios at each contact pressure investigated, it is seen that contact resistance increases due to the anodized coating range from 27% to 45% for SEM heat sinks and from 22% to 64% for ISEM heat sinks. This effect is worthy to remember when attempting to optimize conduction interfaces for application to cooling electronic modules.

TABLE 5-1

UNANODIZED SEM

Altitude (ft)	Average Combined Surface Finish (μin)	Contact Pressure (PSI)	θ (^{o}C/Watt)
Sea Level	69	25	5.11
		50	4.01
		100	3.47
		150	3.00
10,000	69	25	5.31
		50	3.95
		100	3.44
		150	3.08
30,000	69	25	5.67
		50	4.26
		100	3.57
		150	3.29
50,000	69	25	5.93
		50	4.54
		100	3.84
		150	3.39
80,000	69	25	6.19
		50	4.83
		100	4.03
		150	3.55

TABLE 5-2

ANODIZED SEM

Altitude (ft)	Average Combined Surface Finish (μin)	Contact Pressure (PSI)	θ (^{o}C/Watt)
Sea Level	90	25	6.27
		50	4.62
		100	4.66
		150	4.20
10,000	90	25	6.61
		50	4.81
		100	4.74
		150	4.40
30,000	90	25	7.41
		50	5.61
		100	4.94
		150	4.58
50,000	90	25	8.04
		50	5.84
		100	5.55
		150	4.94
80,000	90	25	8.46
		50	6.67
		100	6.06
		150	5.53

TABLE 5-3

UNANODIZED ISEM

Altitude (ft)	Average Combined Surface Finish (μin)	Contact Pressure (PSI)	θ (°C/Watt)
Sea Level	73	25	3.99
		50	2.76
		100	1.85
		150	1.57
10,000	73	25	4.04
		50	2.78
		100	1.85
		150	1.59
30,000	73	25	4.21
		50	2.94
		100	1.89
		150	1.71
50,000	73	25	4.45
		50	3.06
		100	2.00
		150	1.71
80,000	73	25	4.79
		50	3.20
		100	2.12
		150	1.81

TABLE 5-4

ANODIZED ISEM

Altitude (ft)	Average Combined Surface Finish (μin)	Contact Pressure (PSI)	θ (^{o}C/Watt)
Sea Level	77	25	4.88
		50	2.93
		100	2.86
		150	2.38
10,000	77	25	5.03
		50	3.28
		100	2.81
		150	2.50
30,000	77	25	5.42
		50	3.51
		100	2.98
		150	2.65
50,000	77	25	5.79
		50	3.81
		100	3.29
		150	2.87
80,000	77	25	6.40
		50	4.51
		100	3.92
		150	3.43

TABLE 5-5

RATIO OF ANODIZED TO BARE ALUMINUM GUIDE RIB INTERFACE RESISTANCE

SEM

	25 PSI	50 PSI	100 PSI	150 PSI
Sea Level	1.23	1.15	1.34	1.40
10K Feet	1.24	1.22	1.38	1.43
30K Feet	1.31	1.32	1.38	1.39
50K Feet	1.36	1.29	1.44	1.46
80K Feet	1.37	1.38	1.50	1.56

ISEM

	25 PSI	50 PSI	100 PSI	150 PSI
Sea Level	1.22	1.06	1.55	1.52
10K Feet	1.25	1.18	1.52	1.57
30K Feet	1.29	1.19	1.58	1.55
50K Feet	1.30	1.25	1.65	1.68
80K Feet	1.34	1.41	1.85	1.90

SECTION VI

THEORETICAL ANALYSIS OF EFFECTS OF REDUCED ATMOSPHERIC PRESSURE ON FORCED-AIR FILM COEFFICIENTS

6.0 INTRODUCTION

When examining the difference in thermal performance of forced-air cooled electronic equipment between sea-level and high altitude conditions, there are two basic phenomenon that may reduce thermal performance relative to sea-level conditions: (1) non-continuum rarefied gas effects that retard heat transport rates from the convecting surface and, (2) changes in the thermophysical properties of air in the continuum flow regime. Section II of this report addressed rarefied gas phenomenon and Section III examined variations in properties of air, so these former sections will be used as a baseline for examining the effects of altitude on forced-air film coefficients.

For the purpose of this report it is assumed that an avionics equipment environmental control system (ECS) provides for the same cooling air mass velocity (ρV) at altitude conditions of 70,000 feet as it does at sea level conditions. In reality, there are many different ECS approaches for coping with the reduced density effects of air at high altitudes (e.g. variable speed fans, reducing temperature of supply air with increasing altitude, etc.), but the scope of this report does not allow a detailed examination of these methods. The basic thrust of this section will be to examine intrinsic thermal degradation as the result of using low density air as a forced-air cooling medium.

6.1 RAREFIED GAS EFFECTS IN FORCED-AIR ELECTRONIC EQUIPMENT COOLING

In order to assess whether conditions for "slip flow" or "free molecular flow" exist in conventional forced-air cooled electronic systems, let us examine a typical cooling situation whereby $15^{o}C$ air at a free-stream velocity of 15 feet per second is flowing over a ceramic chip carrier package 0.2 inches on a side. The air is assumed to be at a density corresponding to that of 70,000 feet altitude as depicted in Table 3-1. In examining equation 2-1 herein, the Knudsen number (Kn) must be evaluated to determine whether conditions for "slip flow" exist. The characteristic physical dimension, L, of equation 2-1 is actually the physical dimension of the chip carrier package. Therefore, the Knudsen number is evaluated as follows:

$$Kn = \lambda m/L = 0.00029$$

Where: $\lambda m = 5.844 \times 10^{-5}$ inches (see Table 3-1)

$L = 0.2$ inches

Since Kn is less than 0.001, conditions for continuum flow exist and rarefied gas effects on the thermal and velocity profiles across the chip carrier package do not have to be considered. It should be noted however that electronic components being forced-air cooled and having a characteristic dimension (length or diameter) of less than approximately 0.058 inch would have to be examined for "slip flow".

It is interesting to note that, for the above cooling situation, air velocity has no impact on assessing whether continuum flow or "slip flow" conditions exist. This is true only for low Reynolds number flows as typically exist in the forced-air cooling of electronic equipment whereas, at high speed flows, the Knudsen number is evaluated in terms of Mach number and Reynolds number per equation 2-2 herein.

6.2 FORCED-AIR COOLING PENALTIES DUE TO AIR PROPERTY VARIATIONS

The forced-air convective film coefficient, h, is normally related to the properties of air (or most other gaseous mediums) through empirical expressions containing the Reynolds number (Re) and the Prandtl number (Pr). Table 6-1 reveals the classical dependency that the film coefficient (h) has on the properties of air for various situations involving both laminar and turbulent heat transfer within ducts and over planar surfaces. The specific properties of air contained in these expressions involve the density (ρ), the viscosity (μ), specific heat (Cp), and thermal conductivity (k). Because this analysis assumes the mass velocity of the air does not change when traversing from sea level to 70,000 feet altitude conditions, the ρV term in the Reynolds number is unaffected by altitude. Also, by denoting the values for viscosity, specific heat, and thermal conductivity in Table 3-1, it is seen that there is no change in these properties between sea level and 70,000 feet for the same temperature of air. As a result it can be concluded that, for the same air mass velocity at sea level and 70,000 feet altitude, the heat transfer film coefficient (h) will virtually be unaffected. This assumes, of course, that the ECS provides the same temperature air at 70,000 feet as at sea level. If, in fact, air temperatures are different, the use of air property equations from Section III in conjunction with Table 6-1 will allow a quick evaluation of the effects of varying temperature.

6.3 PRESSURE DROP PENALTIES AT ALTITUDE CONDITIONS

The assumption of having the same mass velocity of air at 70,000 feet altitude as at sea level can have dramatic effects on static pressure losses over heat exchanger surfaces. Considering air flowing in a duct, the static pressure loss across a given heat exchange surface is expressed as follows, using the classical fluid mechanics relationship:

$$\Delta P = f \frac{L}{D} \frac{\rho V^2}{2G_c} \qquad \text{(equation 6-1)}$$

Where: ΔP = Pressure loss

f = Friction factor

L = Length of viscous shear surface

D = Hydraulic diameter of viscous shear surface

ρ = Density of fluid

V = Fluid velocity

G_c = Gravitational constant

For laminar flow in a duct, the friction factor (f) is proportional to 1/Re and for turbulent flow f is proportional to $1/Re^{0.2}$. Noting the assumption that mass velocity (ρV) is constant between sea level and high altitude conditions, the Reynolds numbers at sea level and 70,000 feet are identical for a given air temperature and, therefore, the friction factors are identical. Thus, considering the same heat exchange surface configuration and equal air mass velocities, the static pressure loss ratio between altitude and sea level may be expressed as follows.

$$\frac{\Delta P_{ALT}}{\Delta P_{SL}} = \frac{\rho_{SL}}{\rho_{ALT}} = \frac{V_{ALT}}{V_{SL}} \qquad \text{(equation 6-2)}$$

Equation 6-2 was derived from equation 6-1 by considering that ρV = constant ($\rho_{ALT} V_{ALT} = \rho_{SL} V_{SL}$) and performing the proper substitution of terms. Thus, it is seen from equation 6-2 that the pressure loss increase due to altitude is simply the density ratio. Table 6-2 shows the static pressure loss ratios at various altitudes relative to sea level conditions. It is easily seen that a thermal designer must size flow passages based on equipment operation at altitude conditions in order to keep the pressure head, against which air moving devices must operate, at a reasonable level. When selecting an air moving device which must operate at both sea level and high altitude conditions, consideration should be given to using a high slip or constant torque motor which will keep the mass flow of air relatively constant regardless of air density changes. Conventional airmovers deliver the same volume flow of air at high altitude as at sea level and can effect severe thermal performance penalties at altitude and high motor loading at sea level.

TABLE 6-1

EMPIRICAL CORRELATION PROPORTIONALITIES FOR FORCED-AIR FILM COEFFICIENTS

Cooling Situation	Empirical Formula
Laminar Flow in a Tube or Duct	$h \propto \frac{k}{D}(Re\ Pr)^{1/3}(\frac{D}{L})^{1/3}$
Turbulent Flow in a Tube or Duct	$h \propto \frac{k}{D} Re^{0.8}\ Pr^{0.33}$
Laminar Flow Over Flat Plate	$h \propto \frac{k}{D} Re^{0.50}\ Pr^{0.33}$
Turbulent Flow Over Flat Plate	$h \propto \frac{k}{D} Re^{0.8}\ Pr^{0.33}$

h = Forced air film coefficient

Re = $\rho VD/\mu$

Pr = $C_p \mu / k$

k = Thermal Conductivity

D = Characteristic dimension or hydraulic diameter

TABLE 6-2

PRESSURE LOSS RATIOS FOR EQUAL MASS FLOW

Altitude (ft)	Pressure Loss Ratio ($\Delta P_{ALT} / \Delta P$ Sea Level)
Sea Level	1.00
10,000 ft	1.45
30,000 ft	3.35
50,000 ft	8.79
70,000 ft	23.18

SECTION VII

COMPARISON OF THEORETICAL AND EMPIRICALLY-DERIVED INTERFACE THERMAL RESISTANCES

7.0 INTRODUCTION

The theoretical results (based on the application of the "V" correlation) of Section IV and the empirical results of Section V will be compared in this section for the case of the anodized ISEM guide rib thermal interface. The results presented on the "V" correlation are representative of conditions whereby perfect alignment exists between an anodized ISEM guide rib and an anodized card guide surface at a combined surface finish of 125 microinches (62 microinches on guide rib and 62 microinches on card guide). The empirical results presented are representative of conditions whereby a somewhat imperfect alignment exists (due to macro-roughness or waviness) between an anodized ISEM guide rib and a bare (but oxidized) aluminum card guide surface at a combined average surface finish of 77 microinches. The 125 microinch combined surface finish was chosen instead of a 65 microinch finish for the "V" correlation due to macroroughness or warp possibilities in the empirical (77 microinch) test set-up.

7.1 COMPARISON OF THEORETICAL AND EMPIRICAL RESULTS

Figure 7-1 reveals the theoretical results of the thermal interface resistance for an anodized ISEM guide rib with varying contact pressure and altitudes between sea level and 70,000 feet. Figure 7-2 reveals the empirical results of the thermal interface resistance for an anodized ISEM guide rib under the same variable conditions except that altitudes up to 80,000 feet are examined. Comparison of Figures 7-1 and 7-2 shows a surprisingly good correlation between the experimental and theoretical data. The correlation of

data is excellent between contact pressures of 50 and 150 PSI whereas a departure is noted between 25 and 50 PSI. The empirical data of Figure 7-2 reveals that thermal interface resistance is a much stronger function of contact pressure between 25 and 50 PSI than does the theoretical data of Figure 7-1. It is likely that the theoretical model established by using the "V" correlation does not offer much resolution in the 25-50 PSI contact pressure range due to lack of data at these lower pressures. As a result, the departure of the data between 25 and 50 PSI, as evidenced by comparing Figures 7-1 and 7-2, may be somewhat expected. It is suggested by this author that in the 25-50 PSI range the data for the empirical results be used for thermal predictions in lieu of the theoretical results.

If one superimposes Figure 7-1 onto Figure 7-2, it is seen that the slopes of the curves in the range of 50-150 PSI are nearly identical suggesting the same dependence of interface resistance on contact pressure. This is encouraging and supports the conclusion drawn in Section IV that thermal interface resistance is only a moderate function of contact pressure for the contact pressure range studied.

7.2 EFFECT OF ALTITUDE ON ISEM THERMAL INTERFACE RESISTANCE

Table 7-1 shows both the theoretical and empirically derived effects of altitude on an ISEM guide rib thermal interface. It is seen that between sea level and 70,000/80,000 feet, increases in thermal resistances range from roughly 30% to 50% relative to sea level thermal resistance values. Based on conclusions reached in Section IV it is expected that for surface finishes smoother than those studied for this specific case even larger percentage-wise increases will result, and conversely, for rougher surface finishes smaller

percentage-wise increases in thermal interface resistances will result. Although the increases in thermal resistances do not match exactly when comparing theoretical with empirical data, the range of increases (31%-47% versus 31%-54%) correlate rather well. In assessing the general effect of increasing altitude on thermal interface resistance, the results of this study offer a considerable confidence level in the ability to predict the behavior of thermal interface at given altitude conditions based on the availability of only sea level thermal data.

TABLE 7-1

EFFECT OF ALTITUDE ON THERMAL INTERFACE RESISTANCE

Contact Pressure	Percent Increase in Interface Resistance	
	Theoretical*	Empirical**
25	47%	31%
50	43%	54%
100	36%	37%
150	31%	44%

* Increase Between Sea Level and 70,000 Feet

** Increase Between Sea Level and 80,000 Feet

THEORETICAL RESULTS-ANODIZED ISEM INTERFACE RESISTANCE

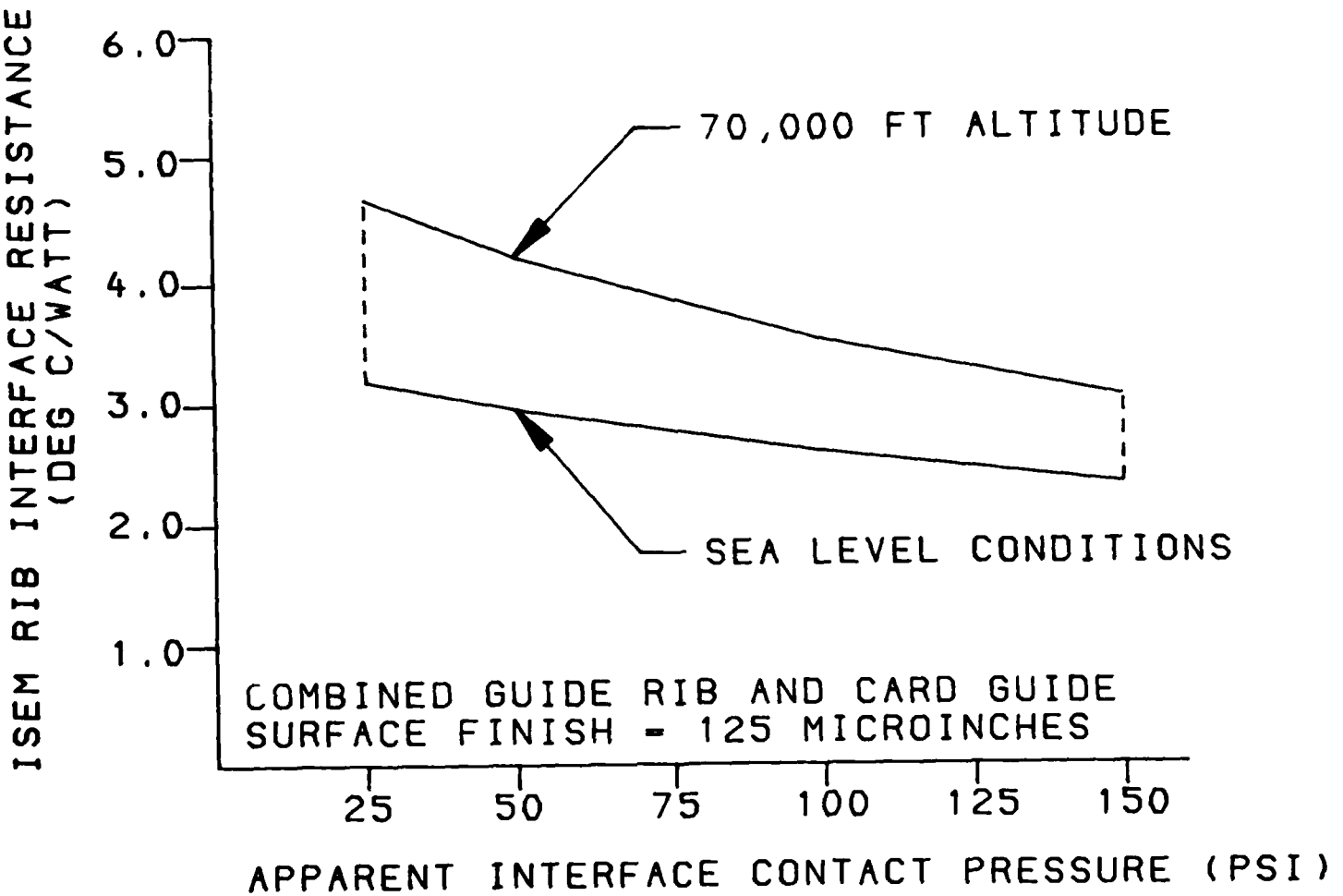

FIGURE 7-1

EMPIRICAL RESULTS-ANODIZED ISEM INTERFACE RESISTANCE

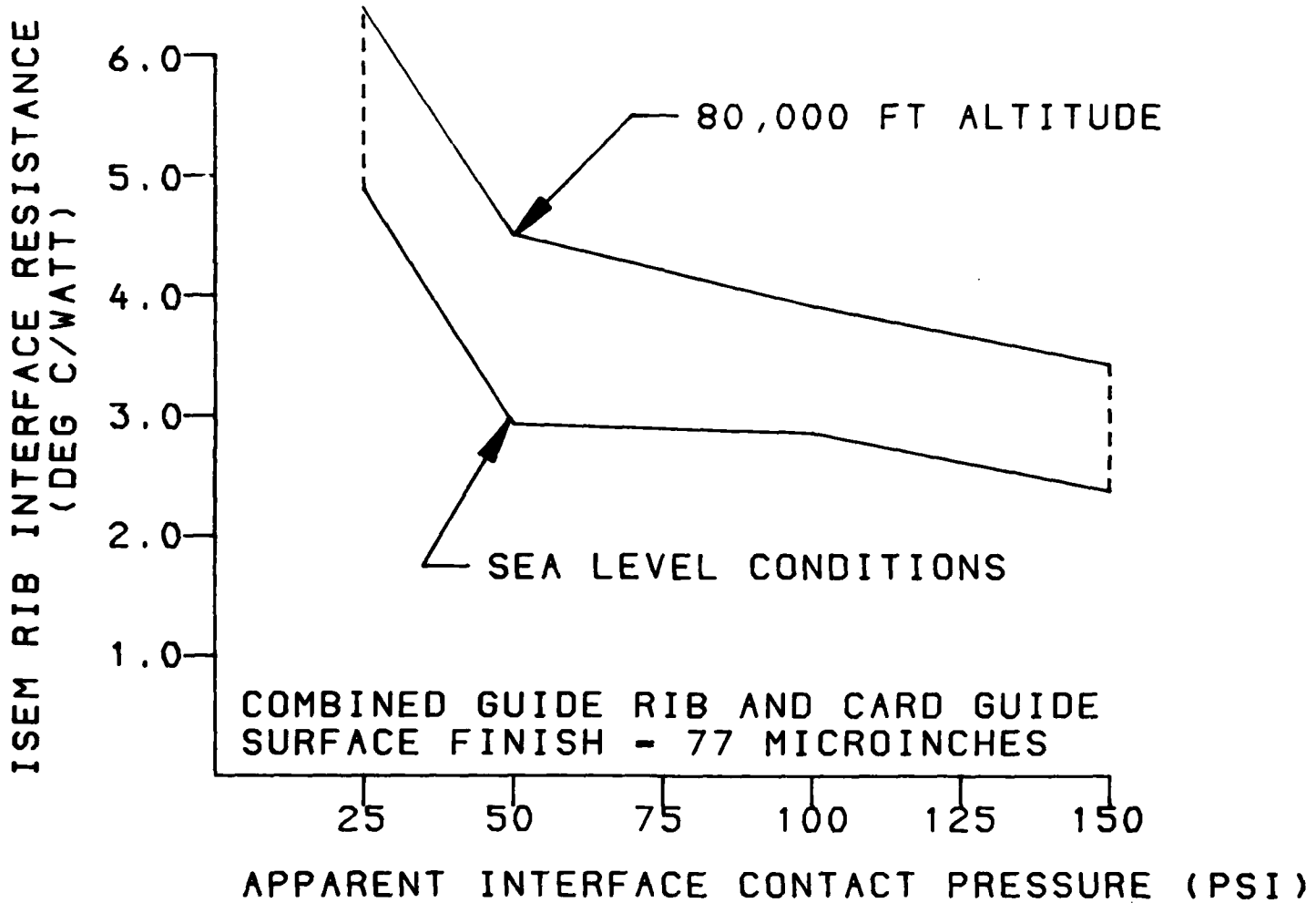

FIGURE 7-2

SECTION VIII

REFERENCES

1. Holman, J. P., "Heat Transfer", Second Edition, McGraw-Hill, 1968

2. Rohsenow, W. M. and Hartnett, J. P., "Handbook of Heat Transfer", McGraw-Hill, 1973

3. McAdams, W. H., "Heat Transmission", Third Edition, McGraw-Hill, 1954

4. "U. S. Standard Atmosphere", 1962

5. Veziroglu, T. N, "Correlation of Thermal Contact Conductance Experimental Results", Prog. Astron. Aero., 20, Academic Press, Inc., New York, 1967

6. Leaght, V. E. and DeBellis, A., "Hardness Testing Handbook", U.S.A., 1969